Low-temperature magnetic properties of the ferromagnetic organic radical, *p*-nitrophenyl nitronyl nitroxide

Y. Nakazawa, M. Tamura, N. Shirakawa, D. Shiomi, M. Takahashi, M. Kinoshita, and M. Ishikawa
Institute for Solid State Physics, the University of Tokyo, Roppongi Minato-Ku Tokyo 106, Japan
(Received 3 March 1992)

Low-temperature magnetic properties of the β and γ phases of *p*-nitrophenyl nitronyl nitroxide (*p*-NPNN) were determined by measuring the specific heat, the magnetic susceptibility, and the hysteresis curve of magnetization above ^{3}He temperature in external magnetic fields. The β-phase crystal undergoes a bulk ferromagnetic transition at 0.60 K, which was confirmed by the magnetic entropy of R ln2 due to one unpaired electron on the radical molecule and the hysteresis curve. The γ phase, on the other hand, revealed an antiferromagnetic transition at 0.65 K and one-dimensional ferromagnetic fluctuations above it. The specific-heat data of the γ phase in external fields were analyzed by a mean-field theory incorporated in the one-dimensional Heisenberg model. The details of sample characterization of each phase based on thermal analysis are also given.

I. INTRODUCTION

Magnetic properties of organic free radical substances have attracted much attention from both the experimental and theoretical sides because these substances, having a variety of molecular structures and crystal symmetries, often provide an ideal Heisenberg system with various space dimensionality and magnetic coupling. Several materials, such as TANOL suberate, BDPA, and DPAN, were studied as model systems of a low-dimensional magnet.[1-3] The former two materials behave as a one-dimensional system with the exchange constant ratio $|J'/J| \simeq 0.1$ and 0.05, respectively, and DPAN is known as a two dimensional antiferromagnet. These substances exhibit a hump in the specific-heat curve characteristic of the short-range order of a low-dimensional magnet and some most often undergo three-dimensional antiferromagnetic long-range order at a lower temperature. In organic radical materials, a ferromagnetic intermolecular coupling is quite rare as compared with an antiferromagnetic one. Although several substances such as galvinoxyl radical[4-6] and TANOL suberate radical[1] are known to possess a positive paramagnetic Curie temperature, they do not fall into a ferromagnetically ordered state, but into a nonmagnetic dimerized or a long-range antiferromagnetic state. The search for a bulk ferromagnetic substance composed only of light elements such as H, C, N, and O has been one of the most challenging problems in this field of material science. Several groups have recently reported ferromagnetism at room temperature in some organic polymers consisting of light elements,[7] but a too small saturation moment and poor reproducibility left the problem unsettled.

On the other hand, *p*-nitrophenyl nitronyl nitroxide ($C_{13}H_{16}N_3O_4$), abbreviated as *p*-NPNN, is a unique organic radical in the sense that all of the four metamorphic phases (α, β, β_h, and γ) are supposed to possess a ferromagnetic intermolecular coupling.[8-10] In particular, the largest positive paramagnetic Curie temperature was reported for the γ phase by Turek *et al.* and a possibility of ferromagnetic long-range order was suggested for this phase.[10] According to their suggestion, we recently studied the γ phase down to about 0.4 K by means of specific-heat and susceptibility measurements and reported that this phase undergoes a three-dimensional ferromagnetic order at 0.65 K and behaves as a quasi-one-dimensional Heisenberg ferromagnet with $J=4.3$ K above the transition.[11,12] Soon the β phase was also found to transform into a long-range ferromagnetic state at 0.60 K, as is briefly reported elsewhere.[13] However, our subsequent careful investigations on these phases of *p*-NPNN have revealed that the ferromagnetism previously reported for the γ phase did not actually occur in this phase but occurred in the adulterated sample with an improper β phase which a part of γ phase transformed into during the experiment. The transition at 0.65 K in the proper γ phase turned out to be of long-range antiferromagnetic order. In the course of sample characterization, the γ phase was proved to be one of the metastable high-temperature phases of the β phase and it gradually transformed back to the β phase under certain circumstances. The detailed characterization of both the β and γ phases leading to these findings is reported in this work, together with the thermodynamic and magnetic properties of these phases.

II. SAMPLE CHARACTERIZATION AND EXPERIMENT

Following the discovery of the orthorhombic β phase by Awaga *et al.*,[14] the existence of other phases such as α and β_h was reported by Allemand *et al.*[9] They also reported that the β phase transforms to another β_h phase at 132 °C and the latter melts at 172 °C. The triclinic γ phase was more recently identified by Turek *et al.*[10] The crystallographic data of these phases are summarized in Table I. Structure refinement of the β_h phase has recently been completed and the result will be published else-

TABLE I. The crystallographic data of *p*-NPNN.

	α phase monoclinic ($P2/c$)	β phase orthorhombic ($F2dd$)	γ phase triclinic ($P\bar{1}$)	β_h phase monoclinic ($P2_1/c$)
a (Å)	7.307	12.363	9.193	8.963
b (Å)	7.596	19.364	12.105	23.804
c (Å)	24.794	10.971	6.471	6.728
α	90°	90°	97.35°	90°
β	93.543°	90°	104.44°	104.25°
γ	90°	90°	82.22°	90°

where. The preliminary result is also included in Table I.

p-NPNN (see Fig. 1 for the molecule) was synthesized according to the published procedure in Refs. 15 and 16. Large, dark green, single crystals of the β phase were grown by slow evaporation of a benzene solution of *p*-NPNN. Growth from an acetonitrile solution sometimes yields γ-phase crystals. In order to recognize the appropriate conditions for the formation of each phase, about 40 mg of small crystals of the β and γ phases were analyzed by DTA (differential thermal analysis) in air and the heating curves taken at 3° C/min are displayed in Fig. 1. The two endothermal peaks were observed for the β phase around 100 and 135 °C, whereas for the γ phase only the higher-temperature peak was observed. Above about 170 °C, both of them decomposed into a reddish material. The higher-temperature peak corresponds to the structural phase transformation to the β_h phase reported in Ref. 9. Single-crystal samples of the β phase quenched from 115 and 140 °C turned out to be polycrystalline γ and β_h phases, respectively, although those annealed at 80 °C retained the β structure. It is therefore concluded that the γ phase is an intermediate phase stable in a narrow temperature range between 100 and 130 °C. By choosing appropriate solvents and temperatures of solution, we succeeded in growing large crystals of the β and γ phases weighing about 10–30 mg. Typical conditions appropriate for the β and γ phases are 20 °C from benzene and 60–70 °C from acetonitrile or chloroform, respectively. During a series of experiments, we found that both the γ and β_h phases are not very stable and gradually transform back to the β phase even below room temperature. A single crystal which gave only the Bragg spots attributable to the γ structure on an x-ray oscillation photograph turned to also show the Debye rings due to a randomly oriented mosaic of the β phase after keeping at 10 °C for a few weeks. This tendency is accelerated greatly in prolonged contact with a low-temperature grease such as Apiezon N or Wakefield grease, probably because the surface layers of the crystals get partially damaged by organic solvents in such greases and transform into the β phase. We therefore took special care in handling samples and x-rayed them before and after measurements to verify the state of samples. All samples used in this study were freshly prepared just prior to each measurement.

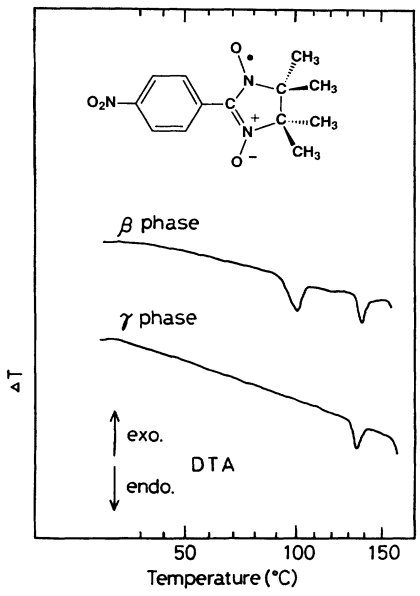

FIG. 1. DTA curves of β- and γ-phase samples heated at 3 °C/min in air and the molecule of *p*-NPNN.

The dc susceptibility was measured in the range of 1.8–300 K with a Quantum Design MPMS SQUID magnetometer. The ac susceptibility was measured on a powdered sample of the γ phase and bulk single crystals of the β phase in the ac field of about 100 mOe at 123 Hz. The data were corrected for the background which was measured without a sample in a separate run. The specific heat was measured by a quasiadiabatic heat pulse method in a ^{3}He cryostat, whose detailed description was previously reported.[17] Magnetization versus magnetic field curves were recorded by an integration technique in which the difference of the voltages induced on pickup and reference coils by sweeping the magnetic field is integrated over time by a computer. The two identical coils were 25 mm long, 5.5 mm in the inner diameter, and 7.6 mm in the outer diameter, in which a 0.03-mm ϕ copper wire is wound with the density of 6×10^3 turns/cm. Changing the sweeping rate of magnetic field did not make a significant difference, but the rate was typically 13 and 90 Oe per sec for the β and γ phases, respectively. The ferromagnetic saturation moment was calibrated with nickel metal.

III. EXPERIMENTAL RESULTS

The dc susceptibilities of the single crystals of the β and γ phases are shown as a function of temperature in Figs. 2(a) and 2(b). The susceptibilities below 4.5 K were taken at 500 Oe to minimize the saturation effect as much as possible. The product of the paramagnetic susceptibility (χ_p), which was obtained by correcting for the core diamagnetism, and temperature at 300 K amounts to 0.37 emu K mol^{-1} for the β phase and 0.38 emu K mol^{-1} for the γ phase. These values are consistent with the Curie constant for $S=\frac{1}{2}$ originating from one electron on each radical molecule. The paramagnetic Curie temperature determined by fitting the data to the Curie-Weiss law is about 1.2 K for the β phase and 2 K for the γ phase, sug-

gesting that ferromagnetic coupling is dominant in these phases. However, in the γ-phase sample, the fitted Curie-Weiss curve gradually deviates upwards below about 15 K, while that of the β-phase sample fits well the experimental points in the wider temperature range between 4 and 300 K. In Fig. 2(b), we also compare the data of the γ phase with the theoretical calculation (denoted by the solid curve) based on the ferromagnetic one-dimensional Heisenberg model[18] with an intrachain coupling of $J=4.3$ K. The agreement is much better in the whole temperature range 1.8–300 K than that of the Curie-Weiss fitting (dashed curve). These results indicate that both phases surely possess ferromagnetic coupling and that the γ phase behaves as a quasi-one-dimensional ferromagnet. These high-temperature data prompted us to examine both phases for a long-range magnetic order

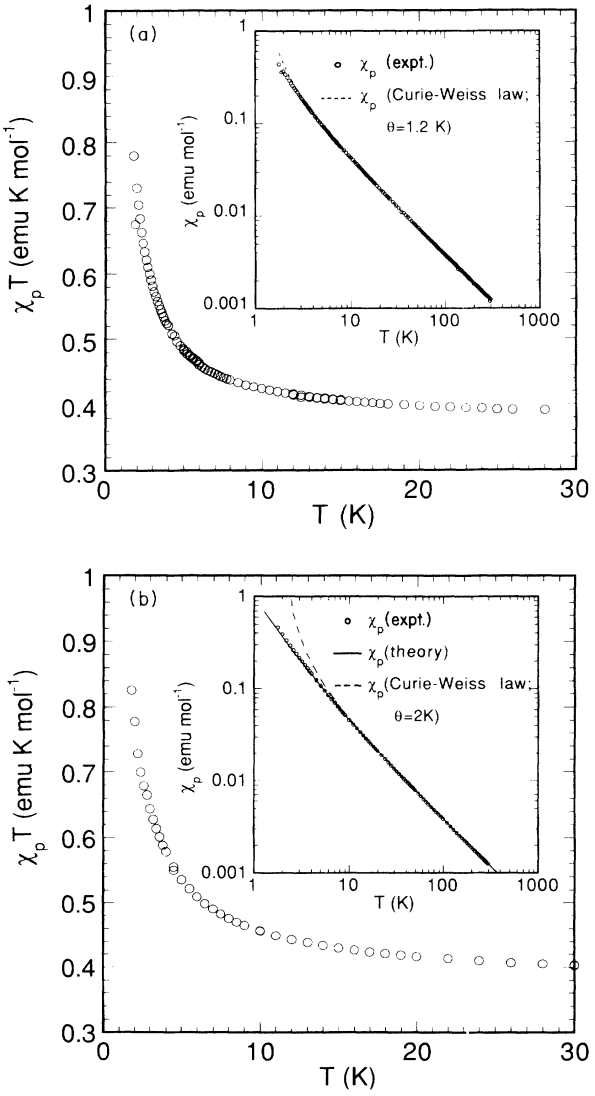

FIG. 2. dc susceptibility multiplied by temperature as a function of temperature for (a) β-phase and (b) γ-phase samples. The insets are log-log plots of χ_p vs T. The solid curve in (b) was calculated by the one-dimensional Heisenberg model with $J=4.3$ K (see text).

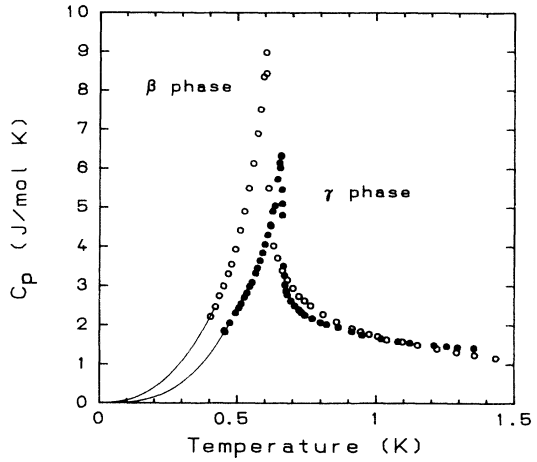

FIG. 3. Zero-field specific-heat curves of γ- and β-phase samples. The smooth curves at the low-temperature end represent the spin-wave approxmation for three-dimensional antiferromagnetic and ferromagnetic systems (see text).

at lower temperatures. We performed the specific heat, ac susceptibility, and magnetization measurements down to about 0.4 K.

The specific-heat measurements on the β and γ phases were performed on freshly prepared single crystals weighing 34.6 and 18.1 mg, respectively. The raw data of these samples were corrected for the heat capacity of 15.7 mg of Apiezon N grease for the β phase and 5.7 mg of Wakefield grease for the γ phase. As shown in Fig. 3, both phases exhibit a sharp λ-like peak at 0.60 and 0.65 K, corresponding to a three-dimensional magnetic phase transition. We compare the specific heat of these phases in a wider temperature range up to 13 K in Fig. 4. The γ phase has a peculiar plateau in the temperature range 1–5 K, which is considered as a contribution of one-dimensional spin fluctuations, as discussed in the next section.

The ac susceptibility data normalized by weight are compared for the β and γ phases in Fig. 5 (to read off the

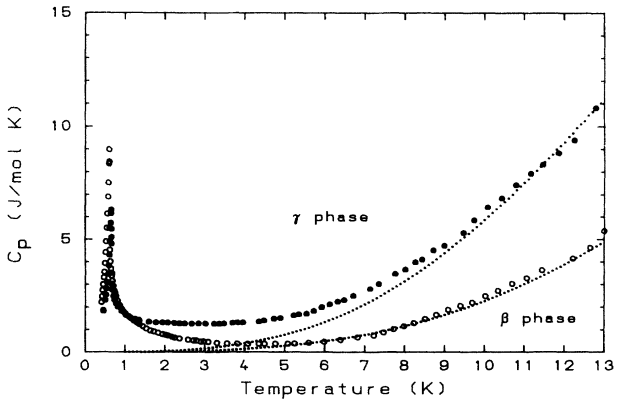

FIG. 4. C_p vs T curves of γ- and β-phase samples between 0 and 13 K. The dotted curves represent the lattice specific-heat calculated by the Debye approximation with $\Theta_D=88.7$ and 140 K for each phase.

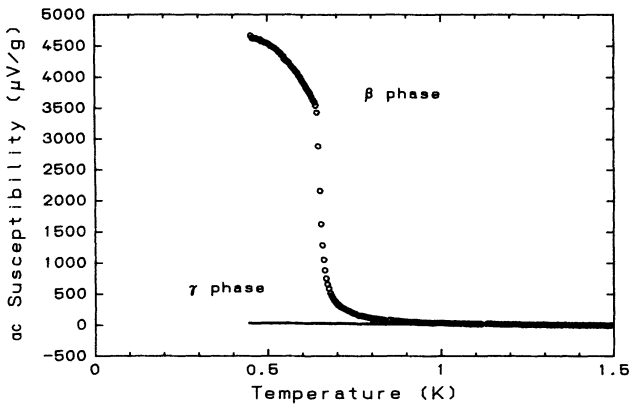

FIG. 5. ac susceptibility of γ- and β-phase samples normalized by weight.

magnitude of the signal for the γ phase, see the zero-field curve in Fig. 7). The unit used here for the ac susceptibility represents the weight-normalized voltage generated in the secondary mutual inductance coil. The β phase displays ferromagnetic behavior evidenced by the upsurge of the susceptibility around 0.60 K. We show some more ac susceptibility curves in static magnetic fields applied perpendicular to the ac field in Fig. 6, which demonstrates that the large susceptibility signal is suppressed by a relatively weak external field of $\sim$500 Oe. Figure 7 displays the ac susceptibility of the γ phase in a transverse field of up to 1800 Oe obtained for 139 mg of a powdered sample. No contamination of the β phase was confirmed by an x-ray powder diffraction within 12 h after the low-temperature measurements. The cusp at 0.65 K just corresponds to the specific-heat peak of the γ phase shown in Fig. 3. This ac susceptibility curve of the γ phase indicates that the phase transition at this temperature is of antiferromagnetic nature. Hence, the upsurge of the susceptibility reported for the "γ" phase in Refs. 11 and 12 around this temperature was due to the β-phase contamination as explained in the previous sections.

Figure 8 shows the isothermal magnetization curves of

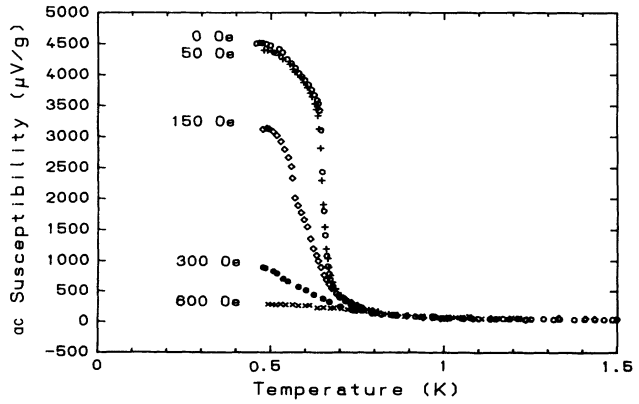

FIG. 6. ac susceptibility of single crystals of the β phase under the static field of 0–600 Oe applied perpendicular to the ac field.

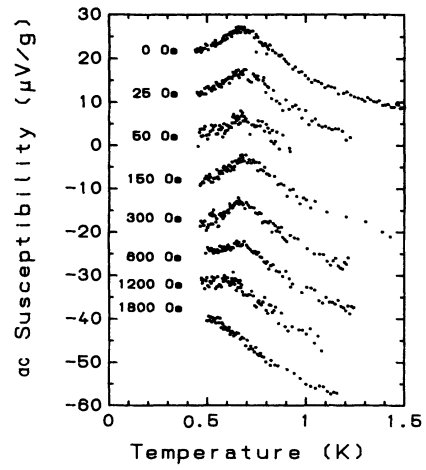

FIG. 7. ac susceptibility of powdered samples of the γ phase under the field of 0–1800 Oe. Each curve for a finite field is consecutively shifted by 10 μV/g with increasing field.

these phases below and above their phase transition. The β-phase specimens were six prism-shaped bars with the long axis aligned parallel to the sweeping field. For determining the demagnetization factor (D), each bar was regarded as a prolate spheroid having the real cross-sectional area of the bar at the equator. Thus calculated polar-to-equatorial axes ratios of the six bars averaged 5.8, from which D of 0.045 was derived. Considering that the long axis was parallel to the applied field, D must

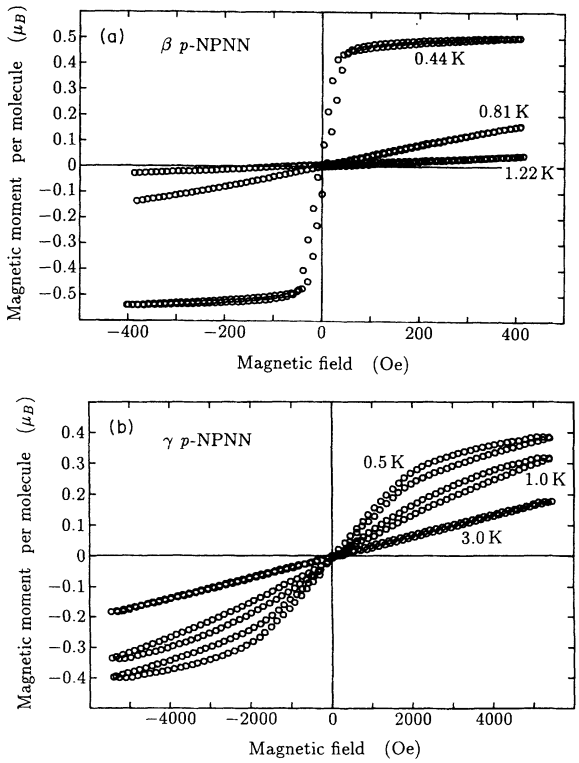

FIG. 8. Isothermal magnetization curves of (a) β-phase and (b) γ-phase samples at various temperatures.

be small and the ambiguity in the value of D is not crucial to determining the magnetic moment. The β phase shows a hysteresis loop [Fig. 8(a)] at 0.44 K characteristic of ferromagnetism, which has a saturation field of 50 Oe and a small coercive force. The small coercive force and saturation field are considered as the result of a small spin-orbit coupling and anisotropy in this phase (see also Sec. IV). The saturation moment ($0.5\mu_B$ per molecule at 0.44 K) is too small to be accounted for by the general temperature dependence of the saturation moment M_s; that is, $M_s(T)/M_s(0)\sim 0.8$ at $T/T_c=0.73$.[19] The observed $0.5\mu_B$ is only 50% of the $M_s(0)=1.0\mu_B$ expected for one unpaired electron per molecule and this may be characteristic of the delocalized nature of the electron over each molecule. It is, in fact, interesting to note that the hysteresis loop of this compound resembles very much that of an itinerant electron ferromagnet $ZrZn_2$,[20] notwithstanding our organic radicals are insulating. It would be important to obtain the precise saturation moments $M_s(0)$ by determining its temperature dependence down to lower temperatures. At the temperature of 0.81 or 1.22 K higher than the Curie temperature, a linear

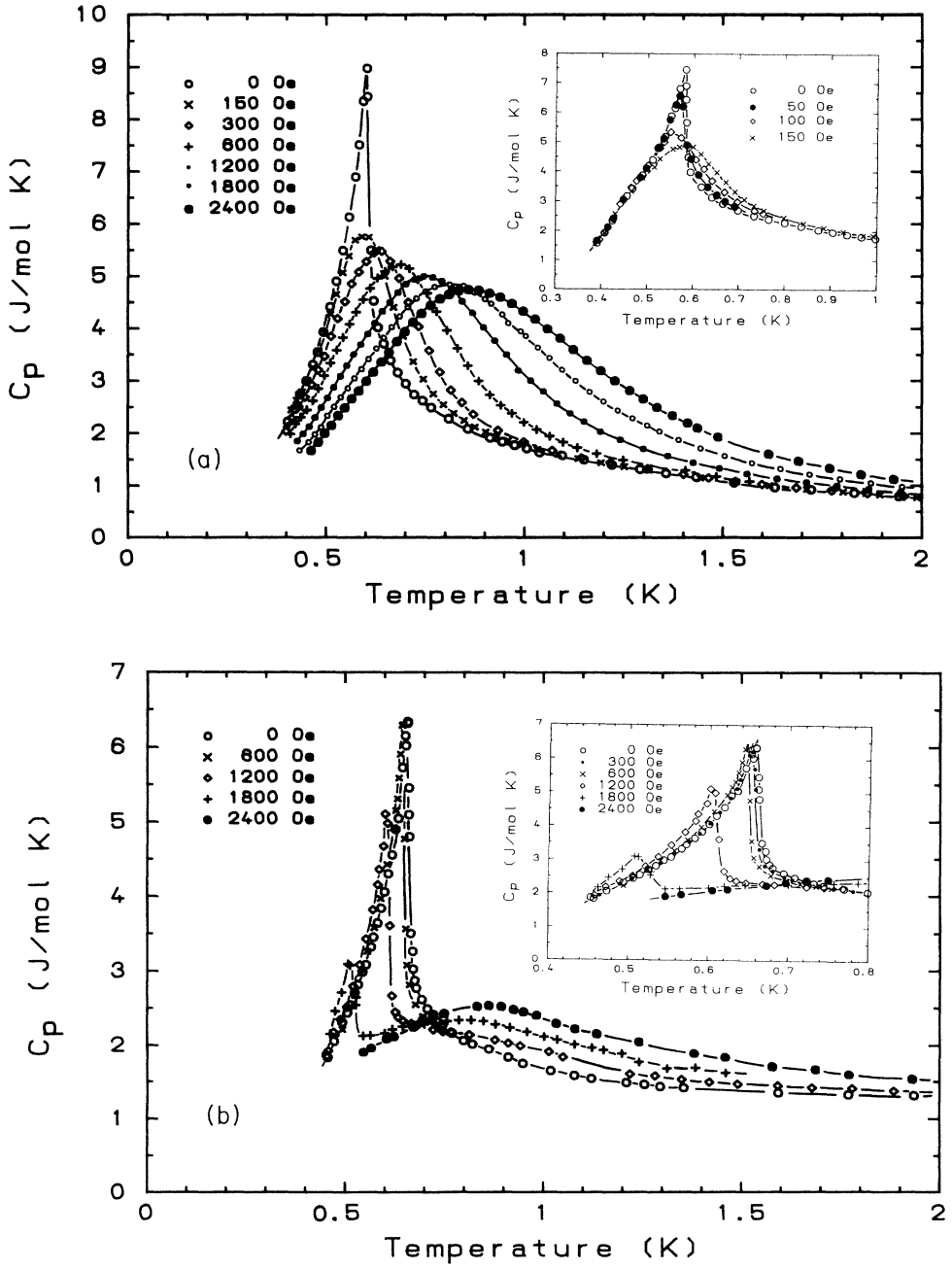

FIG. 9. (a) Specific-heat curve of the β phase under the static field of 0–2400 Oe applied parallel to the b axis. The inset shows the low-field (0–150 Oe) behavior for a different sample with $T_c=0.57$ K. (b) Specific-heat curve of the γ phase under the static field of 0–2400 Oe applied perpendicular to the bc plane.

magnetization curve indicative of the paramagnetic state manifests itself.

The curve for the γ phase [Fig. 8(b)] on the other hand, contrasts remarkably with that of the β phase. In the ordered state at 0.5 K, the magnetization increases almost linearly up to about 2000 Oe, where a break of the slope is noticeable on the curve. This field corresponds to the critical field at which the antiferromagnetic to paramagnetic transition takes place. The cause of the hysteresis observable for the 0.5- and 1.0-K curves is not yet clear. We cannot rule out the possibility that it is only an experimental artifact, but it might be related to the slow magnetization process of this phase.

Although the zero-field specific-heat curves near the phase transition are very much alike for the β and γ phases (see Fig. 3), the magnetic field dependence is rather different, as shown for fields between 0 and 2400 Oe in Figs. 9(a) and 9(b). The λ-type peak of the β phase already disappears around 100 Oe and the broadened peak gradually shifts to higher temperatures with the field, while that of the γ phase slightly shifts downward by retaining the shape up to relatively high fields. The gradual suppression of the Néel temperature by an external field is consistent with the ac susceptibility data in the fields shown in Fig. 7.

It is known that, for ferromagnetic substances, the critical temperature cannot be defined in a finite magnetic field, contrary to the antiferromagnetic case. The variation of the specific heat of a ferromagnet in external magnetic fields was theoretically studied by Griffiths in 1969.[21] He suggested that, in low magnetic fields, magnetic domains are formed so as to make the net magnetization $M=(1/D)H_e$, where H_e is an external field and D is the demagnetization factor. In the case of isotropic spin systems, a similar demagnetization is realized by forming a nonuniformly magnetized state even though magnetic domains cannot be formed. In both cases, the internal field expressed by $H_i=H_e-DM$ is nullified below a certain value of H_e and the specific heat in magnetic fields C_H becomes independent of H_e, i.e., coinciding with that in zero field below a certain temperature T^*. T^* is found as the temperature where the spontaneous magnetization M_s is equal to $(1/D)H_e$. Above this temperature, M_s is no longer capable of canceling out H_e and C_H begins to deviate downwards from the zero-field curve. C_H of the β phase shown in Fig. 9(a) is consistent with this interpretation by demagnetization. It is clearly demonstrated in the inset which displays the specific-heat curves in low fields below 150 Oe for another β-phase sample with a slightly lower Curie temperature. Such a field dependence of the specific heat has also been confirmed in EuS (Ref. 22) and $K_2CuCl_4\cdot 2H_2O$,[23] which are known as an isotropic Heisenberg ferromagnet.

IV. DISCUSSION

In organic free radicals, the g factor is usually very close to the free-electron value (2.0023) as compared with that of other magnetic atoms with $S=\frac{1}{2}$. It is the evidence for a negligibly small spin-orbit coupling in these substances. This is also true for p-NPNN: the principal g factors determined by an EPR measurement at room temperature are $g_a=2.0070$, $g_b=2.0030$, $g_c=2.0106$ for the β phase[13] and $g_1=2.0117$, $g_2=2.0051$, $g_3=2.0038$ for the γ phase.[10] From a low-temperature measurement, small temperature dependences of g factors were observed: they vary $|\Delta g/g|<0.05$ at ^{4}He temperature. Thus, the $S=\frac{1}{2}$ isotropic Heisenberg model is most suitable to describe the present system. On the other hand, space dimensionality is sensitively affected by the crystal structure of the metamorphic phases of p-NPNN. Quasi-one-dimensional character has been revealed in the γ phase from the analysis of the dc susceptibility and the specific heat, which has the lowest crystal symmetry (triclinic) among the four known phases of p-NPNN (see Table I).

Bonner and Fisher[24] have studied the thermal properties of the one-dimensional $S=\frac{1}{2}$ Heisenberg model with both ferromagnetic and antiferromagnetic coupling. They calculated $N=2-11$ spin systems and inferred the behavior expected for the case of $N\rightarrow\infty$. Decades ago Bethe[25] demonstrated that the exact many-body wave function of the one-dimensional Heisenberg Hamiltonian can be written down analytically. Using his formalism, one of the authors (Takahashi) and his co-workers derived the coupled integral equations which determine the thermodynamic quantities of this system.[26] The specific heat and magnetic susceptibility at finite temperatures can be calculated by this set of equations.[18] It was found that the susceptibility diverges as T^{-2} and that the specific heat behaves as $\sqrt{T}$ at low temperatures. These low-temperature properties are also explained by the modified spin-wave approximation.[27] More recently, thermodynamic properties were calculated by applying the Bethe ansatz technique to the quantum transfer matrix (not to the Hamiltonian).[28] Using this method we can precisely calculate thermodynamic quantities such as the magnetization curve, magnetic susceptibility, specific heat, and correlation length up to six or seven significant figures at a given temperature. The Hamiltonian is

$$\mathcal{H}=-J\sum_{i=1}^{N}\mathbf{S}_i\cdot\mathbf{S}_{i+1}-2h\sum_{i=1}^{N}S_i^z\ , \tag{1}$$

where $h=g\mu_B H/2$, $S=\frac{1}{2}$. The free energy of this system per spin $f(T/h)$ is given by the following equation for a series of complex numbers, p_l ($l=1,2,3,\ldots$):

$$f(T,h)=-T\ln 2-\frac{T}{2}\sum_{l=1}^{\infty}\ln\left\{\frac{(1+p_l^2)(1+\bar{p}_l^{\,2})}{[4\pi T(l-1/2)/J]^4}\right\}\ , \tag{2}$$

where

$$p_l=\frac{4\pi T}{J}(l-\tfrac{1}{2})+\frac{4hi}{J}+\frac{p_l}{1+p_l^2}+\frac{2T}{Ji}\sum_{j=1}^{\infty}\ln[L(p_l,p_j)L(p_l,-\bar{p}_j)]\ , \tag{3}$$

$$L(x,y)=\frac{1-(1-ix)^{-1}+iy}{1-(1+ix)^{-1}+iy} . \quad (4)$$

It has been shown that this set of equations is equivalent to the thermodynamic Bethe ansatz integral equations.[26] At $l \gg J/T$, p_l approaches $4\pi T(l-\frac{1}{2})/J+\text{const}\times i$. So we can determine the p_l's at a given T and h by iteration. The magnetization, energy, susceptibility, and specific heat are obtained by differentiation of the free energy and p_l's. The numerical calculations of these equations are straightforward. The derivation of Eqs. (2)–(4) in the case $h=0$ is given in Ref. 28 as a special case of XYZ chains. The equation of the XXZ chains in a nonzero field as the generalization of Eq. (2) is given in a separate paper.[29]

In order to compare the specific-heat data with this theoretical calculation for the $S=\frac{1}{2}$ system, the magnetic specific heat must be separated from the measured C_p. The lattice specific heat C_l was estimated by assuming the Debye approximation. The Debye temperature Θ_D was determined to be 88.7 and 140 K for the γ and β phases by minimizing the standard deviation of $\Delta C=C_p-C_l$ in the temperature ranges of 10–18 K and 5–13 K. These low values of the Debye temperature are commonly found in organic materials, for example, $\Theta_D=91$ K for TANOL suberate,[1] 83.5 K for DPAN,[3] and 52.5 K for BDPA.[2] The difference in the crystal structure and the density of the β and γ phases may explain such a difference in their Debye temperature (1.41 and 1.34 g/cm^3 calculated for β and γ, respectively). The magnetic specific heat C_{mag}, determined as ΔC, is shown in Fig. 10. The magnetic entropy S_{mag} was calculated by integrating C_{mag}/T with respect to temperature and shown in Fig. 11. The low-temperature part of the C_{mag} curves is determined by extrapolating the experimental curve with the three-dimensional spin-wave approximation, namely, with a sum of $T^{3/2}$ and $T^{5/2}$ terms for the ferromagnetic β phase and a T^3 term for the antiferromagnetic γ phase (see also Fig. 3). The magnetic entropy up to 10 K amounts to 92 and 89% of R ln2 for the β and γ phases, respectively. This almost full entropy, which is consistent with the attribution of $S=\frac{1}{2}$ per molecule inferred above from the value of the Curie constant indeed substantiates the bulk nature of these magnetic phase transitions.

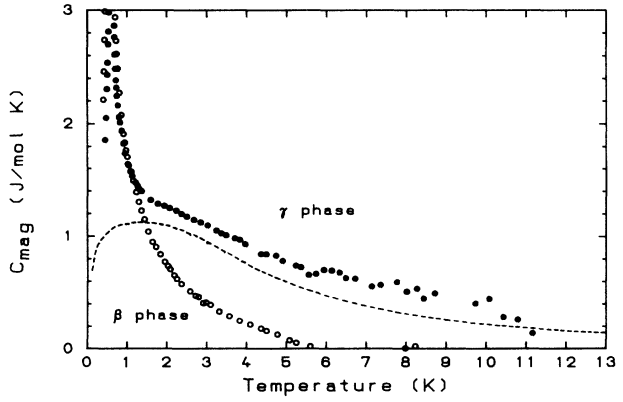

FIG. 10. Magnetic specific heat (C_{mag}) of γ- and β-phase samples. The dashed curve is the theoretical result of a one-dimensional Heisenberg ferromagnet assuming $J=4.3$ K.

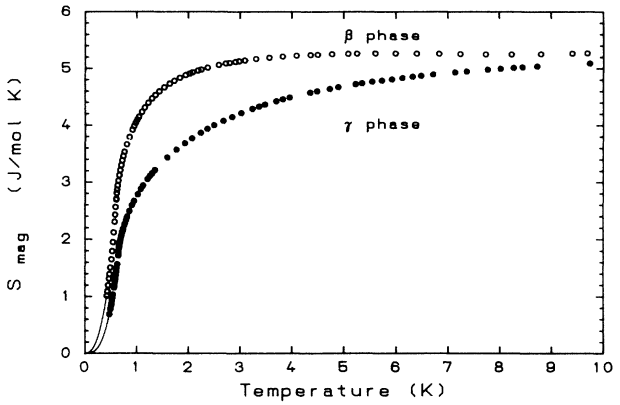

FIG. 11. Temperature dependence of magnetic entropy of the γ and the β phases obtained by integrating C_{mag}/T over temperature.

We now turn to the temperature dependence of the entropy curves of Fig. 11. The entropy of the β phase rises very steeply above the Curie temperature ($T_c=0.60$ K) like an ordinary ferromagnet, and reaches 85% of R ln2 at 2 K, while that of the γ phase increases much more slowly above the Néel temperature ($T_N=0.65$ K). This gradual increase is due to large magnetic specific heat distributed over the wide temperature region above its T_N, which is displayed in Figs. 4 and 10. This excess magnetic entropy above 1.6 K, amounting to about 41% of the total, represents the short-range order which is characteristic of a one-dimensional Heisenberg system. This is corroborated by a theoretical calculation of the magnetic specific heat of a ferromagnetic Heisenberg chain with $J=4.3$ K. The calculated specific heat is shown by the dashed curve in Fig. 10, which qualitatively reproduces C_{mag} except at the low-temperature part below about 1 K, where the three-dimensional antiferromagnetic order sets in as a result of weak interchain coupling. Evidence for the one-dimensional character in this γ phase is more clearly disclosed in the specific-heat curve in high magnetic fields as discussed in the following [see Figs. 9(b) and 13].

The magnetic field dependence of the specific heat of the γ phase can be analyzed in the framework of a mean-field approximation. We assume that ferromagnetic Heisenberg chains have interchain couplings J' and J'':

$$\mathcal{H}=-J\sum \mathbf{S}_r\cdot\mathbf{S}_{r+\delta}-J'\sum \mathbf{S}_r\cdot\mathbf{S}_{r+\delta'} -J''\sum \mathbf{S}_r\cdot\mathbf{S}_{r+\delta''}-2h\sum S_r^z , \quad (5)$$

where δ is the unit vector along the chain direction, while δ' and δ'' are the other lattice vectors. By the mean-field theory for such a linear chain,[30,31] the staggered susceptibility χ_s, is given by

$$\chi_s=\frac{\chi_0}{1-(1/2)(|J'|+|J''|)\chi_0} , \quad (6)$$

and the phase transition temperature is determined by

$$1=\tfrac{1}{2}(|J'|+|J''|)\chi_0 , \tag{7}$$

where χ_0 is the susceptibility of a pure one-dimensional Heisenberg model ($-\partial^2 f/\partial h^2$). By using the experimentally determined values of $J=4.3$ K and $T_N=0.65$ K, and $\chi_0=5.08$, which was obtained by the numerical calculation of thermodynamic equations, we get

$$|J'|+|J''|=0.4 \text{ K} . \tag{8}$$

On the other hand, the critical field h_c is determined by the following equations:

case 1,

$$(|J'|+|J''|)m(T,h_c/2)=h_c \quad \text{for } J',\ J''<0 , \tag{9}$$

case 2,

$$|J''|m(T,h_c/2)=h_c \quad \text{for } J'>0,\ J''<0 , \tag{10}$$

case 3

$$h_c=0 \quad \text{for } J',J''>0 . \tag{11}$$

In Ref. 11, we analyzed the system assuming case 3, but in the present extended model case 3 should be excluded because the phase transition occurs at a finite magnetic field. In case 1 or 2, the system can have antiferromagnetic long-range order below some critical temperature. When a uniform external field is applied, the sublattice magnetizations are almost perpendicular to the external field. The calculated critical field is given for cases 1 and 2 in Fig. 12. The best fit of the experimental values of h_c (denoted by solid circles) was obtained for case 2 with $J'=0.244$ K and $J''=-0.176$ K. In Fig. 13, we show the specific-heat curves calculated at several external fields for a quasi-one-dimensional Heisenberg Hamiltonian with interchain couplings J' and J''. It can be seen that the calculated curves reproduce very well the experimental curves shown in Fig. 9(b). It is particularly interesting to note that the calculation demonstrates the way in which the magnetic field tends to suppress the antiferromagnetic interchain coupling and disclose the one-dimensional ferromagnetic fluctuations around 1 K in high fields.

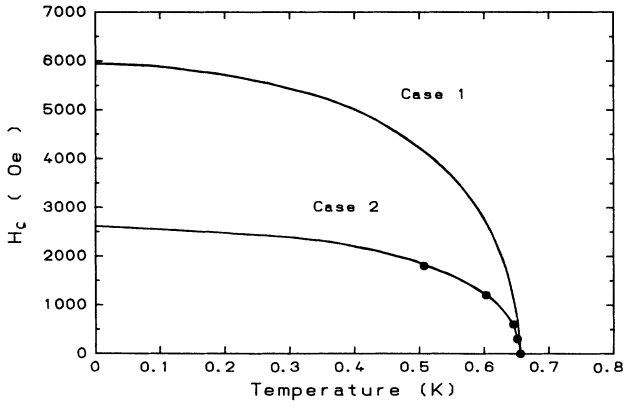

FIG. 12. Theoretical and experimental transition temperatures at a fixed magnetic field. The upper curve is the result of case 1 where $J',J''<0$ and $J'+J''=-0.4$ K. The lower curve is case 2 where $J'=0.224$ K and $J''=-0.176$ K. The solid circles are experimental transition temperatures for a fixed magnetic field.

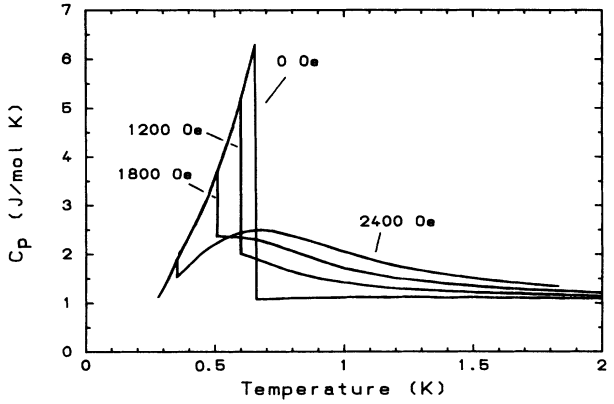

FIG. 13. Theoretical magnetic specific heat of a quasi-one-dimensional Heisenberg ferromagnet with $J=4.3$ K, $J'=0.224$ K, and $J''=-0.176$ K. The interchain couplings were determined by the mean-field approximation.

The three-dimensional coupling constant J of the β phase was estimated from the following three formulas:

$$\Theta=\frac{2zS(S+1)}{3}\left[\frac{J}{2}\right] , \tag{12}$$

$$\frac{C_{\text{mag}}T^2}{R}=\frac{2zS^2(S+1)^2}{3}\left[\frac{J}{2}\right]^2 , \tag{13}$$

$$\frac{E}{R}=zS^2\left[\frac{|J|}{2}\right] , \tag{14}$$

where Θ is the paramagnetic Curie temperature and E is the magnetic energy obtained by integrating C_{mag} over temperature. Equations (12) and (13) are obtained as the first terms of the high-temperature expansion of the Heisenberg model. Since the three-dimensional exchange paths in this phase are not well known yet, we assume that the magnetic interaction between molecules is mainly determined by the exchange couplings with the neighboring four molecules in the *ac* plane (first-nearest neighbors) and that with four molecules in the neighboring planes (second-nearest neighbors). So the coordination number z in Eqs. (12)–(14) is assumed to be 8 in our calculation. Using the paramagnetic Curie temperature $\Theta\simeq 1.2$ K for the β phase estimated from the dc susceptibility data, we find from Eq. (12) $J=0.60$ K. The values of J determined by Eqs. (13) and (14) using the magnetic specific-heat data shown in Fig. 10 were found to be 0.76 and 0.53 K, respectively. Therefore, we may conclude from this analysis that J for the β phase is about 0.6 K. It is important to note here that the β and γ phases of *p*-NPNN have quite a different set of intermolecular couplings: $J\simeq 0.6$ K for the β phase and $J\simeq 4.3$ K, $J'\simeq 0.22$ K, and $J''\simeq -0.18$ K for the γ phase. This means that coupling constants between molecules in these organic crystals very sensitively depends on the intermolecular distance and direction. Ferromagnetic coupling seems to

be dominant compared with antiferromagnetic one in the present organic radical, *p*-NPNN.

V. CONCLUSION

In the course of our investigation on magnetic properties of an organic radical *p*-NPNN, we have found that three different phases (β, γ, and β_h) exist between room temperature and 172 °C. The γ phase is found to be an intermediate phase of the β and β_h phases, and is stable in the narrow temperature range between 100 and 130°. Because of the weak spin-orbit coupling inferred from EPR measurements, the magnetism of these phases caused by unpaired electrons on free radicals is well described by the ideal isotropic $S=\frac{1}{2}$ Heisenberg model with different space dimensionality. The β phase undergoes a three-dimensional ferromagnetic transition at 0.60 K, which is the first observation of bulk ferromagnetism in organic substances only consisting of light elements like H, C, N, and O. This phase can be characterized as a three-dimensional Heisenberg ferromagnet with nearest-neighbor coupling $J\simeq 0.6$ K. The very sensitive magnetic field dependence of ac susceptibility and specific heat and the extremely small coercive force in the hysteresis loop are peculiar features of this ferromagnetic phase. These features seem to be characteristic of organic radicals in which unpaired electrons are delocalized over each radical. The γ phase, on the other hand, behaves as a quasi-one-dimensional Heisenberg ferromagnet with $J\simeq 4.3$ K, $J'/J=0.05$, and $J''/J=-0.04$. The interchain coupling of J'' makes this phase transform into a long-range antiferromagnetic state at 0.65 K and above this temperature the one-dimensional characters distinctly manifest themselves, for example, in the specific heat and the susceptibility. In order to further investigate the interesting magnetism of these organic radicals, more precise experiments such as magnetization, dc susceptibility around the phase transition, and neutron diffraction are now underway.

ACKNOWLEDGMENTS

The authors are grateful to Dr. P. Turek and Dr. K. Awaga for valuable discussions and Dr. H. Sawa and Professor R. Kato for the structure refinement of the β_h phase. They also thank Professor S. Ogawa for informing them about the *M-H* data on $ZrZn_2$.

[1]Cl. Jeandey-Veyret, J. Phys. (Paris) **42**, 875 (1981).
[2]W. Duffy, Jr., J. F. Dubach, P. A. Pianetta, J. F. Deck, D. L. Strandburg, and A. R. Miedema, J. Chem. Phys. **56**, 2555 (1972).
[3]W. Duffy, Jr., D. L. Standburg, and J. F. Deck, Phys. Rev. **183**, 567 (1969).
[4]K. Mukai, Bull. Chem. Soc. Jpn. **42**, 40 (1969).
[5]K. Awaga, T. Sugano, and M. Kinoshita, Solid State Commun. **57**, 453 (1986); J. Chem. Phys. **85**, 2211 (1986); Chem. Phys. Lett. **128**, 587 (1986); **141**, 540 (1987); Synth. Met. **27**, B631 (1988).
[6]M. Kinoshita, Mol. Cryst. Liq. Cryst. **176**, 163 (1989).
[7]Yu. V. Korshak, A. A. Ovchinnikov, A. M. Shapiro, T. V. Medvedeva, and V. N. Spektor, Pis'ma Zh. Eksp. Teor. Fiz. **43**, 309 (1986) [JETP Lett. **43**, 399 (1986)]; J. B. Torrance, S. Oostra, and A. Nazzal, Synth. Met. **19**, 709 (1987); A. A. Ovchinnikov and V. N. Spector, *ibid.* **27**, B615 (1988); M. Ota, S. Otani, and M. Igarashi, Chem. Lett. 1183 (1989); H. Tanaka, K. Tokuyama, T. Sato, and T. Ota, *ibid.* 1813 (1990).
[8]K. Awaga and Y. Maruyama, Chem. Phys. Lett. **158**, 556 (1989); J. Chem. Phys. **91**, 2743 (1989).
[9]P.-M. Allemand, C. Fite, G. Srdanov, N. Keder, F. Wudl, and P. Canfield, Synth. Met. **41-43**, 3291 (1991).
[10]P. Turek, K. Nozawa, D. Shiomi, K. Awaga, T. Inabe, Y. Maruyama, and M. Kinoshita, Chem. Phys. Lett. **180**, 327 (1991).
[11]M. Takahashi, P. Turek, Y. Nakazawa, M. Tamura, K. Nozawa, D. Shiomi, M. Ishikawa, and M. Kinoshita, Phys. Rev. Lett. **67**, 746 (1991).
[12]M. Kinoshita, P. Turek, M. Tamura, K. Nozawa, D. Shiomi, Y. Nakazawa, M. Ishikawa, M. Takahashi, K. Awaga, T. Inabe, and Y. Murayama, Chem. Lett. 1225 (1991).
[13]M. Tamura, Y. Nakazawa, D. Shiomi, K. Nozawa, Y. Hosokoshi, M. Ishikawa, M. Takahashi, and M. Kinoshita, Chem. Phys. Lett. **186**, 401 (1991).
[14]K. Awaga, T. Inabe, U. Nagashima, and Y. Maruyama, J. Chem. Soc. Chem. Commun. 1617 (1989); 520 (1990).
[15]D. G. B. Boocock and E. F.Ullman, J. Am. Chem. Soc. **90**, 6873 (1968).
[16]E. F. Ullman, J. H. Osiecki, D. G. B. Boocock, and R. Darcy, J. Am. Chem. Soc. **94**, 7049 (1972).
[17]M. Ishikawa, Y. Nakazawa, T. Takabatake, A. Kishi, R. Kato, and A. Maesono, Solid State Commun. **66**, 201 (1988).
[18]M. Takahashi and M. Yamada, J. Phys. Soc. Jpn. **54**, 2808 (1985); M. Yamada and M. Takahashi, *ibid.* **55**, 2024 (1986); P. Schlottmann, Phys. Rev. Lett. **54**, 2131 (1985).
[19]C. Kittel, *Introduction to Solid State Physics*, 5th ed. (Wiley, New York, 1976), p. 463.
[20]S. Ogawa and N. Sakamoto, J. Phys. Soc. Jpn. **22**, 1214 (1967).
[21]R. B. Griffiths, J. Appl. Phys. **40**, 1542 (1969).
[22]E. Scheer, H. Claus, J. Wosnitza, and H. v. Löhneysen, Phys. Rev. B **40**, 5208 (1989).
[23]A. R. Miedema, H. van Kempen, and W. J. Huiskamp, Physica **29**, 1266 (1963).
[24]J. C. Bonner and M. E. Fisher, Phys. Rev. **135**, A640 (1964).
[25]H. Bethe, Z. Phys. **71**, 205 (1931).
[26]M. Takahashi, Prog. Theor. Phys. **46**, 401 (1971).
[27]M. Takahashi, Prog. Theor. Phys. Suppl. **87**, 233 (1986); Phys. Rev. Lett. **58**, 168 (1987); Jpn. J. Appl. Phys. Suppl. **26-3**, 869 (1987).
[28]M. Takahashi, Phys. Rev. B **43**, 5788 (1991), and references cited therein.
[29]M. Takahashi, Phys. Rev. B **44**, 12 382 (1991).
[30]D. J. Scalapino, Y. Imry, and P. Pincus, Phys. Rev. B **11**, 2042 (1975).
[31]M. Takahashi, J. Phys. Soc. Jpn. **50**, 1854 (1981).